

2018

Numerical analysis of a non-polymeric double-network composite

Qitong Yao
Iowa State University

Follow this and additional works at: <https://lib.dr.iastate.edu/etd>



Part of the [Engineering Mechanics Commons](#)

Recommended Citation

Yao, Qitong, "Numerical analysis of a non-polymeric double-network composite" (2018). *Graduate Theses and Dissertations*. 16496.
<https://lib.dr.iastate.edu/etd/16496>

This Thesis is brought to you for free and open access by the Iowa State University Capstones, Theses and Dissertations at Iowa State University Digital Repository. It has been accepted for inclusion in Graduate Theses and Dissertations by an authorized administrator of Iowa State University Digital Repository. For more information, please contact digirep@iastate.edu.

Numerical analysis of a non-polymeric double-network composite

by

Qitong Yao

A thesis submitted to the graduate faculty

in partial fulfillment of the requirements for the degree of

MASTER OF SCIENCE

Major: Mechanical Engineering

Program of Study Committee:

Wei Hong, Major Professor

Ashraf Bastawros

Michael Bartlett

The student author, whose presentation of the scholarship herein was approved by the program of study committee, is solely responsible for the content of this thesis. The Graduate College will ensure this thesis is globally accessible and will not permit alterations after a degree is conferred.

Iowa State University

Ames, Iowa

2018

Copyright © Qitong Yao, 2018. All rights reserved.

TABLE OF CONTENTS

	Page
ACKNOWLEDGMENTS.....	iii
ABSTRACT	iv
CHAPTER 1. INTRODUCTION	1
1.1 Double-network Hydrogel.....	1
1.2 Double-network Mechanism Applications.....	3
1.3 Non-Polymeric Double-network Composite.....	5
CHAPTER 2. MODELING AND SIMULATION	7
2.1 Design of the non-Polymeric Composite	7
2.2 Model of the first network.....	9
2.3 Model of the Serpentine network.....	10
2.4 General Simulation Information.....	13
2.4.1 Simulation mesh.....	13
2.4.2 Constraints and boundary conditions.....	13
2.4.3 Damage model	15
2.5 Dimensionless Parameters.....	16
CHAPTER 3. RESULTS AND ANALYSIS.....	18
3.1 Damage Process.....	18
3.2 Simulation Results.....	20
3.2.1 Different failure strain with fixed area fraction	20
3.2.2 Different area fraction with fixed failure strain	21
3.2.3 Combined area fraction and failure strain.....	22
3.3 Concluding Results and Discussion.....	24
CHAPTER 4. CONCLUSION AND FUTURE WORK.....	29
4.1 Conclusion.....	29
4.2 Possible Future Work.....	30
REFERENCES	31

ACKNOWLEDGMENTS

I would like to thank my committee chair and major professor Dr. Wei Hong, and my committee members Prof. Ashraf Bastawros and Dr. Michael Bartlett for their guidance and support throughout the course of this research.

In addition, I would also like to thank my friends, colleagues, the department faculty and staff for making my time at Iowa State University a wonderful experience.

ABSTRACT

Double-network hydrogels have drawn much attention for its combined mechanical properties of high stretchability and high mechanical strength and numerous studies have been conducted on these hydrogels with specific emphasis on gel compositions and mechanisms. Additionally, there are also reports on application of double-network gel mechanisms on macro composites which achieved similar results as in the gels. In this thesis, a series of numerical simulations on designing and tuning of a double-network hydrogel inspired non-polymeric composite formed with a coiled serpentine network acting as the long-chain and a solid plate acting as the short-chain are presented. The simulation results show that the designed non-polymeric double-network composite exhibits a very similar damage process to the double-network hydrogels which confirms the possibility of applying the double-network toughening mechanism to fabricate tough non-polymeric composite. The further analysis of the simulation results also provided a peep into the roles of the various structural parameters of the composite, which may help to improve the understanding of the double-network mechanism and optimize the design.

CHAPTER 1. INTRODUCTION

1.1 Double-network Hydrogel

In pursuance of the replacement of bio-mechanical tissue in human body, it is desirable to have material properties like suitable elastic modulus and high mechanical strength and toughness. As an answer to this, in 2003 Prof. Jian Ping Gong from Hokaido University Japan developed a revolutionary method of obtaining very strong hydrogels by introducing a double-network structure for various hydrophilic polymer chains [1]. Consisting of interpenetrating relatively short and stiff chain network and a much longer and initially coiled chain network and up to 90% water, the double-network hydrogels of such kind immediately drawn much attention from the soft matter researchers for its combined properties of high strength and toughness. The toughness of a double-network hydrogel can be magnitude orders of magnitudes higher than that of a single network hydrogel formed with either polymer network and shows a potential to serve as an alternative of some biological tissues including articular cartilage and connective tissues [2]. By reason of the double-network hydro gel overcame the brittleness of conventional gels, the potential application range of hydrogels was greatly expanded in the aspects of biomedical engineering and smart structures [3 - 5].

As a result of the superior mechanical performance of double-network hydrogel, intensive research has been conducted on the mechanical behavior and toughening mechanism of such hydrogels. Now a consensus has been reached that the elevated strength and toughness is the result of its special damage process. Because of the long chain network

(second network) is initially coiled, it is virtually unbreakable without being straightened and in order to straighten the first network, the short chain network (first network) has to be broken. Therefore the large deformation in vicinity of crack tip would induce the sacrificial breakage of first network bonds, which dissipates a tremendous amount of energy, and when the first work is broken, the second network would still hold the integrity of the structure. A supportive fact is that, although the double-network hydrogel possess a great extensibility and nearly complete recovery [6], a significant hysteresis was found in the first loading cycle of both uniaxial tension and compression loading and unloading tests for double-network hydrogels [7] while such a huge hysteresis was never found in the following cycles. In addition. during the tensile test, it has been observed that some necking zones form and grow in the hydrogel and a plateau region appears in the corresponding loading curve, which could also be attribute to the yielding caused the fragmentation process of first network [6].

To further predicts the intrinsic fracture energy of a double-network hydrogel, it is found to be not enough to use the the classical Lake - Thomas Theory which predicts the the fracture energy of a single networks well [8] by approximating it as $\Gamma_{rubber} \sim Nn^{\frac{3}{2}}l_m U$ where N is the number of chains per volume, n is the number of monomers per chain, l_m is the length of each monomer and U the fracture energy of each monomer [9]. Therefore Tanaka [10] and Brown [11] proposed their own phenomenological fracture model for the double-network hydrogel, which both suggest that the prediction of the consumed energy should involve the comparison of the necking zone size around the crack tip. Furthermore, Wang and Hong proposed another phenomenological model for the damage evolution and pseudo-elasticity of double-network hydrogels, and this model enabled the quantitative prediction of

such gels [12]. In this model, two irreversible damage process of double-network hydrogels : the softening induced by the fracture of the first network and the stretchability limited by the pull out of the second network are described by the evolution of two internal damage variables. In addition, the Mullins effect and the stable necking phenomenon are also captured by this model as a significant amount of energy are dissipated in these process which is directly related to the high toughness of double-network hydrogels.

1.2 Double-network Mechanism Applications

While a great amount of research interest was attracted by the superior mechanical properties of the double-network hydrogel and its potential applications, there were also researches conducted in focus of other types of materials but still utilizing the toughening mechanism of double-network hydrogels. Elastomers are a type of material that has a wide range of applications in various fields for their ability to deform to large and recover strains. However, the deformation reversibility is correlated with stiffness: the unfilled elastomers becomes brittle when the Young's modulus is above ~ 1 to 1.5 MPa. As predicted in the Lake and Thomas model [9], the energy required to break an elastomer is proportional to $N_c^{\frac{3}{2}}$, where N_c is the number of monomers between cross-links. Therefore, as an elastomer gets stiffer it is also more cross-linked and having fewer monomers on each chain, and becomes more brittle. In order to overcome this limitation, many empirical strategies were attempted [13 - 16], however the results are either very limited in certain circumstances or induces undesired change in other aspects.

Drawing an analogy between the elastomers and hydrogels as both materials are soft matters without a well-defined yield stress, Creton group proposed a strategy to strengthen elastomers with the sacrificial bonds [17]. The sacrificial bonds are introduced by fabricating the multi-network elastomer through pre-stretching and sequential polymerization and the pre-stretched first network bonds would break and dissipate energy before the elastomer fails just like in the double-network hydrogel. In addition, they utilized the Chemoluminescent cross-linking molecules to provide real-time tracking of the sacrificial breakage of first network bonds, which could provide more insights towards the molecular level mechanisms of the fracture of soft materials.

Aside from the multi-network elastomer, a highly stretchable double-network composite was also reported by Hong group in 2016 [18]. Inspired by the toughening mechanism of double-network hydrogels, they fabricated the composite with stacked VHB tape and nylon mesh and at certain composition the composite is significantly stronger and tougher than the base materials. In this composite, the nylon mesh plays the role of the first network in double-network hydrogel and the VHB tape serves as the second network. When being partially damaged the nylon mesh breaks into small islands surrounded by highly stretched VHB tapes which is equivalent to the long chain holds the integrity of the hydrogel when the first network breaks. Moreover, the proposed one-dimensional model based on finite sliding at the interface could also be potentially applied to the double-network hydrogels as the loading behavior of this composite possess a similarity to that of the hydrogel.

1.3 Non-Polymeric Double-network Composite

While extensive research has been conducted on the application of the double-network mechanism on polymeric materials, which includes the hydrogels, elastomers and macro elastomer composites [1, 17, 18], the research on applying the double-network idea on non-polymeric material remains very limited. However, the essence of the toughening mechanism of double-network hydrogels, which is the sacrificial breakage of the stiff network, put almost no limits on the material if the fracture sequence can be designated. Therefore, in order to discover the utilization of double-network mechanism on non-polymeric materials, the design and the numerical analysis of a double-network-inspired metallic composite are reported.

Being strong and easy for manufacturing, metals are used nearly everywhere and the ductility of metal allows it to be manufactured into different shapes easily to serve different purposes. However, the stretchability of metals is still limited by deformation localization. On the other hand, metals can be a good candidate of the sacrificial first network material in a double-network composite, since although the toughening mechanism of double-network hydrogels is generally interpreted as the sacrificial breakage, it can also be regarded as the second network relocates the damage inside first network. But this choice brings another question about the selection of second networks. Because the materials more stretchable than metal are normally soft and very compliant, and they may still not be strong enough to withstand the breakage of the metal first network. On the other hand, the stretchability of the material that are strong enough to induce the breakage of metal is often similar to metal or

worse. As an answer to this question, some special structures from reconfigurable materials [19] are considered here.

Reconfigurable materials are materials that allows its structure and physical properties to be dynamically changed in response of various external stimuli [20 - 24]. Recently, a great amount of research interest has been attracted by their wide range of applications [25 - 29]. Among them, there is an increasing interest in designing highly stretchable materials with inspirations from folding based Origami structures [30, 31] and cutting based Kirigami structures [32 - 34]. Since these structures generally increase the stretchability of a material in sacrifice of its strength at small deformation, they are great candidates for the second network. As when metals are designed into such structure to serve as second network, they have the stretchability provided by its special structure and harden to a strength similar to that of metal which allows the delocalization and distribution of the damage. After comparison and evaluation, the serpentine network structure proposed by Ma et al. [35] is chosen over the Kirigami based auxetic structure from Cho et al. [36] for its better capability of the first network materials and ease for modeling.

CHAPTER 2. MODELING AND SIMULATION

2.1 Design of the non-Polymeric Composite

With up to 90vol% of water, a double-network hydrogel carries the applied mechanical load on its interpenetrating polymer networks and these polymer networks are the real inspiration of the double-network composite. The toughening mechanism of the double-network structure is understood as the short chain network would break first and dissipate energy and the long chain network would hold the integrity of the structure when the first network is broken. There are two key points to successfully achieve a similar design: the first point is that the first network requires to be damaged before the second network and the other is the second network should be cross-linked therefore the breakage in the first network would not induce the failure of the structure.

In the double-network hydrogel, the damage sequence is dominated by the structure of the polymer networks: only after the breakage of the short-chain first network, the coiled second network could be straightened and damaged. Inspired by this structure, the non-polymeric composite is designed as a serpentine ligament network backed by a continuum matrix, as shown by Fig. 2.1. Here the serpentine ligament network was chosen over Kirigami-like networks because of the structure of the serpentine ligament network possess more similarities to the long-chain network in the hydrogel and it is believed that a similar mechanism could be achieved. According to the design, the serpentine network will not be straightened until the sacrificial breakage of the filling material and therefore the energy is dissipated. Meanwhile, the serpentine network penetrates the matrix material and the

presentation of a complete damaged cross section without the breakage of the serpentine network is prevented.

While the network-matrix design serves the purpose of a double-network structure, it could be overcomplicated in the aspect of connection between the two components and many possible factors might be considered including bonding, the interfacial contact and sliding after debonding, etc. Here for simplicity, we assume perfect bonding between the two components, so that attention could be paid to the mechanism between the damage interplay between them. If needed, such effects can be included by modeling the interface with cohesive elements. The preliminary model of the composite is simplified into a serpentine network stacked on a block of material as sketched in Fig. 2.1.

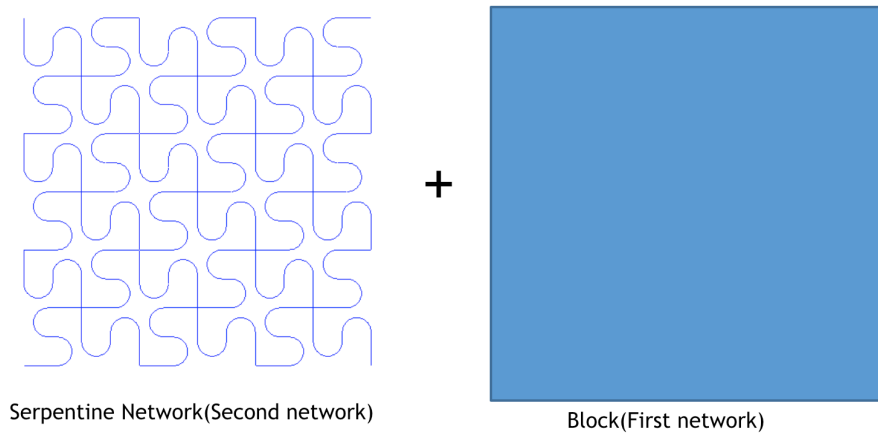


Fig. 2.1 Preliminary model of the composite, consisting of a serpentine network which serves the purpose of the second network as in the double-network gels, and a continuum matrix (the block) which acts as the sacrificial first network. The two components are shown separately for clearer illustration.

2.2 Model of the first network

The first network of the composite prohibits the straightening of the second network and most mechanical energy are dissipated from its sacrificial breakage. According to the design, the continuous and uniform first network could be potentially simplified into a beam when under uniaxial tension prior to damage. However, a beam element is not appropriate for the demonstration of damage propagation in the structure and it fails to integrate the constraints with the serpentine network. Therefore a plane stress element is chosen for balanced simplicity and accuracy to the design.

Besides the geometry of the network, the mechanical properties of the first network are another fundamental part of the model and the mechanical properties of a non-polymeric material may involve its elastic-plastic behavior and its damage behavior. Simulation inputs including modulus, plasticity model and damage model would all affect the mentioned behaviors. However it is unreasonable and unrealistic to manipulate these input parameters simultaneously, which could generate enormous amount of different cases without revealing a clear pattern. Therefore, in the interest of simplicity, the material model of the first network was simplified to highlight its role in the composite and to focus on network interactions.

Table 2.1 First network material model parameters

Modulus	Yield stress	Failure strain
75000 MPa	150MPa	0.2% - 150%

The chosen plasticity model is perfect plastic model, which eliminates the plastic hardening. The yield strain and modulus are immutable to better focus on the damage model of the material. With this plasticity model, the failure stress of the material is also immutable and only the prominent parameter failure strain of the damage model is manipulated which generates the stress-strain curve as shown in Fig. 2.2a. A noteworthy problem is that with the perfect plastic model, the first network block possess a plastic deformation localization in few lines of elements as shown by Fig 2.2b and the failure strain is compiled to be magnified accordingly to approach realistic situations. Therefore the finalized first network material model inputs are as listed in Table 2.1.

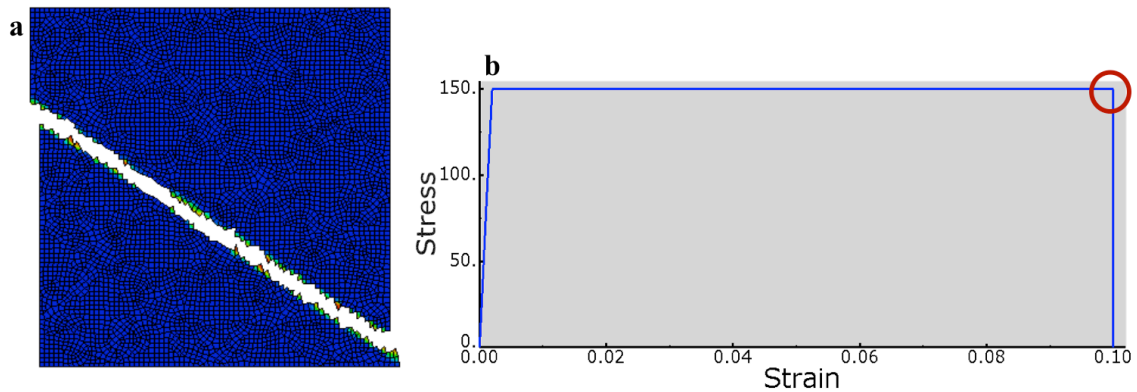


Fig. 2.2 (a) Plastic deformation localization in the first network block. Most elements show no plastic deformation. (b) Stress-strain curve of the first network material model. The manipulated failure strain is circled.

2.3 Model of the Serpentine network

The detailed design of the geometry of the serpentine ligament unit cell with a non-polymeric material is an interesting topic. With a soft polymeric material, the stress concentration at the turning corners can be neglected and the geometry of the unit cell mainly

contribute to the extensibility and the relative modulus of the structure to the material, which together influence the fracture work. However in the non-polymeric situation, the intrinsic characteristic of a metallic material causes earlier hardening and deformation localization inside the serpentine ligaments and the occurrence of these phenomena is significantly affected by the geometry. In fact, the optimization of the structure of the kind with a metallic material requires much more effort and far beyond the scope of this research, hence with careful consideration, we decided that the geometry of the serpentine network unit cell would not be mutated through the study in order to focus on the interaction of two networks and the chosen geometry is shown in Fig 2.1.

The second network of a double-network composite holds the integrity of the structure when the first network is damaged locally and relocates the local damage to undamaged zones. Therefore the damage of the second network indicates the failure of the composite and ends the damage process. However this research focuses on the interaction between two networks during an uniaxial tensile test which is concluded into the first network preventing the straightening of the serpentine network and the serpentine network relocate damage in the first network, hence the damage evolution in the serpentine ligaments especially at the curves is not interested in and perform little contribution to the result. Accordingly, a beam element with aspect ratio of 1 was chosen for finite element analysis to highlight the link character of the serpentine network and accelerate the calculation.

Additionally, the material model of the serpentine network, although important, may not serve as the input parameters of the numerical analysis for several reasons. First it is undeniable that the modulus of the serpentine network is determined by the modulus of the

material, but the ratio of the two modulus of first and second network, which is more important, is always calculated with the two modulus and changing the modulus of first network allows a more direct manipulation over the ratio so the serpentine material modulus was fixed to be 75000 MPa. Second, although a limited failure strain of the material model prohibits the fully straightening of the serpentine ligaments, it contributes little to the extensibility of the structure which is mainly affected by the geometry when the serpentine ligaments can be straightened. Therefore the failure strain of the material model is immutable 50% which is higher than the realistic metallic materials to offset the contribution of out of plane deformation. Finally, despite the fact that the hardening and failure stress have prominent influences on the fracture work of the serpentine structure, the serpentine structure fracture work plays a minor role in the fracture work of the composite. Hence it is unnecessary to include these parameters as simulation variables and the resulted stress strain curve for the fixed material model is presented in Fig. 2.3.

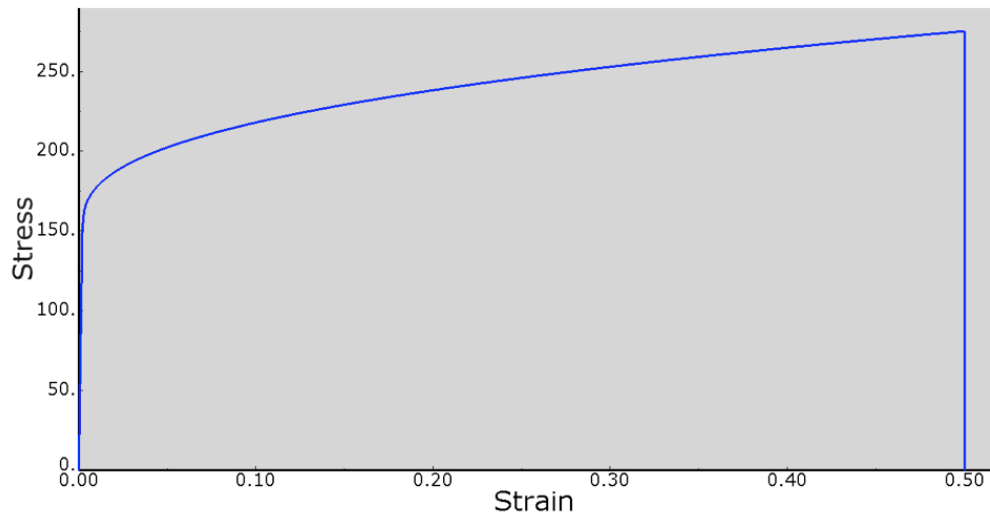


Fig. 2.3 The stress strain curve for serpentine network material model. The yield stress here is 150 Mpa and the failure stress is 270 Mpa.

2.4 General Simulation Information

With the established models of the two networks, the simulation was carried out with the commercial finite element package SIMULIA Abaqus 6.14. Some other inputs beside the two models will be introduced in the following sections.

2.4.1 Simulation mesh

A finite element method generally discretize the complex physical system into small domains called element and through solving equations over these elements the behavior of the system is predicted. Hence the mesh influences both the accuracy and the complexity of the simulation directly. A more refined mesh normally improves the accuracy of the simulation but produces a heavier computational load and it is important to balance the two. Here for this research, the mesh was refined times to minimize the mesh dependency of the result and the mesh was generated automatically in Abaqus with a characteristic length of the elements is $1/3$ of the radius of the serpentine curvature as shown in Fig. 2.4 (a). There are 72 elements on each edge and totally 1224 beam elements and 6285 plane stress elements are assigned to the serpentine network and first network accordingly.

2.4.2 Constraints and boundary conditions

In finite element analysis, the connection between two different parts are applied through constraints, which are user defined functions describing the relationship between the status of the affected nodes. According to the model of this design, the bonding is assumed to

be perfect between the first and second network. Therefore a tie constraint that regulates the displacements to be same between tied nodes in all degree of freedoms is applied.

The boundary conditions are the known value of displacements or loads that required for solving equations over nodes. Since in this research, a uniaxial tensile test was carried, which generally requires the most basic boundary conditions, a simple set of boundary conditions are applied as shown in Fig. 2.4 (b). The boundary condition for the nodes on the bottom edge is ENCASTRE, which implies that the node displacements in all degree of freedom are 0 and the boundary condition for the nodes on top edge is a displacement $u_y = kt$, where t is the time. The coefficient k is also adjusted to avoid the dependency of strain rate and the strain rate for simulation is therefore set to be 0.015% per second.

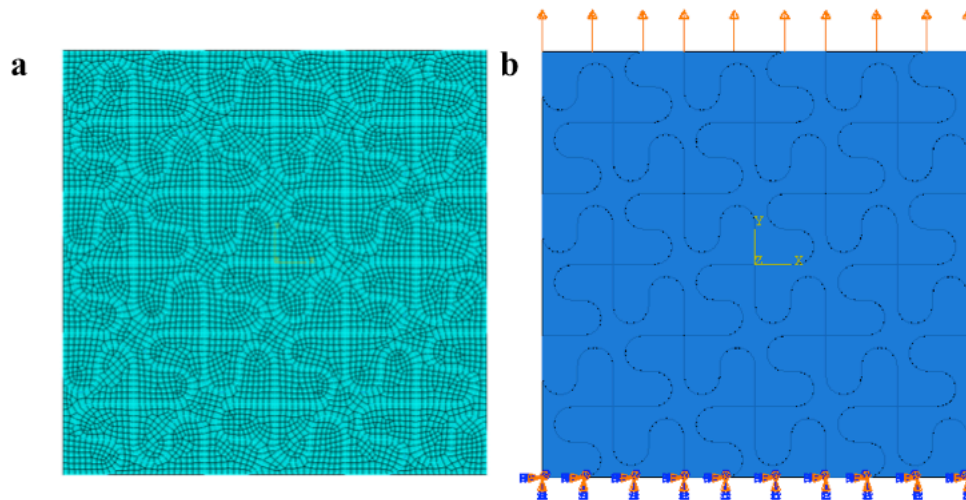


Fig. 2.4 (a) The mesh for input geometry. There are 72 elements on each edge.(b) The illustration of boundary conditions. The top one is a positive time dependent displacement in y-direction and the bottom one is no displacement in all directions.

2.4.3 Damage model

The damage model includes the damage initiation and the damage evolution of a material and should be part of the material model. However, because of the damage models in the simulation for the two networks have a high degree of similarity, they are introduced together.

The damage initiation defines the point of initiation of degradation of stiffness induced by deformation. Different damage initiation criteria are offered in Abaqus and these criteria can be combined to specify the initiation of damage. In the carried simulation of the double-network composite, the two networks both have simple loading conditions with simple material models and therefore a simple failure strain dominated damage initiation criteria is prescribed to the two material models.

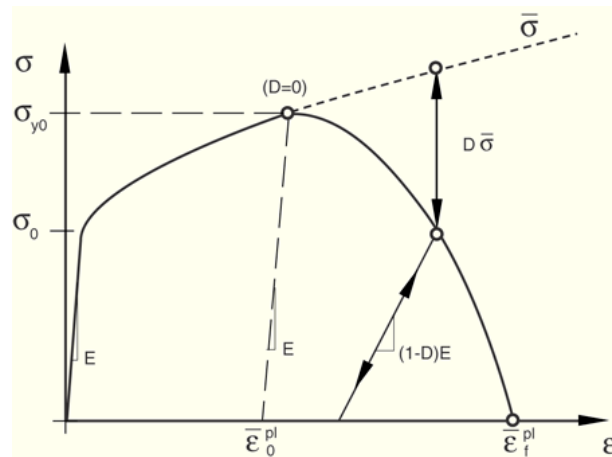


Fig. 2.5 Schematic representation of the effect of the progressive damage model. The dashed line indicates the curve without damage model and D is the damage coefficient captures the effects of all active damage mechanisms. (Adopted from SIMULIA Abaqus User's Manual)

The damage evolution describes the degradation of the material stiffness after the initiation criterion is satisfied. In Abaqus, the damage evolution as represented in Fig. 2.5 is expressed with a formulation based on scalar damage approach, $\sigma = (1 - D)\bar{\sigma}$, where D is the damage variable captures the effects of all active damage mechanics and $\bar{\sigma}$ is the material response in absence of the damage model. Additionally, the change of damage variable D is defined by user through the plastic displacement of element rather than the plastic deformation. The plastic displacement is used because of it involves the characteristic length of elements so that the mesh sensitivity of damage evolution can be minimized.

2.5 Dimensionless Parameters

To study the interaction between two networks of the double-network composite, the variables affecting the composition require to be controlled to reveal the roles of these parameters and with an immutable design and model of the serpentine network, these parameters are all applied to the model of first network. Based on the fact that double-network composite combines the strength of the first network and the extensibility of the second network, two dimensionless variables denote the relationships of the two networks in these two aspects are proposed.

The variable one is the failure strain EF of the first network material. Because of the serpentine network geometry is fixed, the failure strain is proportional to ratio of the ductility of the first network to the extensibility of the serpentine network. The variable two is the cross-sectional area fraction AF of the first network and this fraction is calculated as $A_{first}/(A_{first} + A_{second})$ and ranged from 0% to 60%. While the cross-sectional area of the

second network is constant and the geometry of the first network would not change, the A_{first} is directly proportional to the assigned thickness of plane stress elements of the first network. Furthermore, in consequence of the elegance of the numerical study, change of the thickness of the element is same as the proportional change of the modulus and yield stress of the material model. Therefore this area fraction actually implies the fraction of the strength of the first network in the composite strength. Therefore these two parameters together should cover most network combinations in aspect of extensibility and strength, and the research on how these two variables influence the fracture work of the composite should potentially be able to provide general guidance to future designs of similar composites.

CHAPTER 3. RESULTS AND ANALYSIS

3.1 Damage Process

The damage process of the double-network composite involves the damage initiation inside the composite and the propagation of this damage and the analysis of the damage propagation should promote the understanding towards network interaction. Meanwhile, as the study of the damage process in double-network hydrogels provides the explanation towards the toughening mechanism of the gel, the analogy between the damage process of the two should support the evaluation of double-network composite designs and the damage process of an efficient design should pose a high similarity to that of the gel.

During the uniaxial tensile test simulation, the damage would always be initiated in the first network as a result of the huge difference in extensibility of the two networks and as the progressive damage of the first network, its modulus reduces accordingly causing a clear drop of reaction force as shown in the loading curve in Fig. 3.1. This drop would sustain until the first network cracks into islands that are solely connected by the second network and these strips of second network ligaments in the damage zone will be straightened and loaded until the reaction force exceeds the damage initiation force in the first network islands and the islands would crack into smaller ones. Then this process would repeat till the first network is completely damaged which means the size of first network islands are comparable to that of the serpentine ligaments and the extensibility difference caused by the serpentine structure disappears. After the first network is fully broken, the second network is further loaded and straightened which causes the crack initiation in serpentine network and failure of

the composite. This stage is reflected in the loading curve as a similar hardening of the serpentine network only curve in Fig. 3.1.

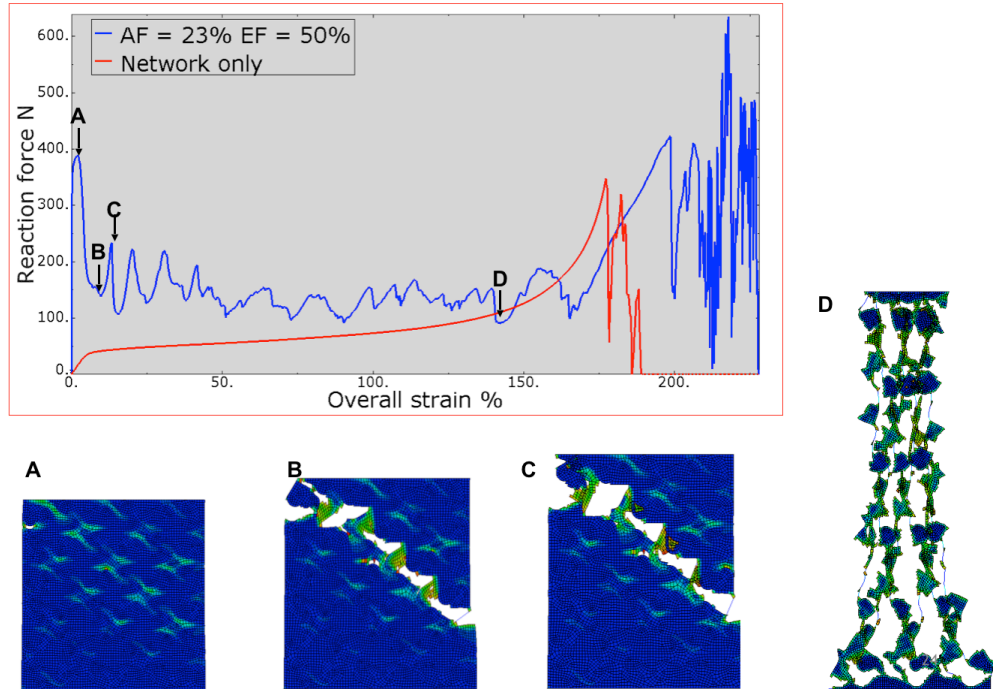


Fig. 3.1 The loading curve from the tensile test simulation for the composite with area fraction 23% and failure strain 50%. The corresponding curve for serpentine network only is also provided here as a reference. A through D are different stages of the damage process. A is the damage initiation in first network, B is the serpentine network in damage initiation zone is straightened, C is the damage relocation and D is the hardening of serpentine network.

Undoubtedly the damage process of the non-polymeric double-network composite presented here has a good agreement with the proposed toughening mechanism. The damage of serpentine network only appears after the complete damage of first network and the second network relocates the local damage to the entire structure, hence an obvious increase in fracture work of the composite is observed. But there is one unexpected phenomenon

during the damage process of first network which is proven to play an important role in the interaction of the two dimensionless parameters. This phenomenon is that as a result of the inhomogeneous deformation distribution in first network, parts of the first network would remain on serpentine network after being damaged and strengthen the serpentine network. Therefore, a fraction of the reaction force required to relocate the damage is carried by these survived fragments of first network, where the relocation force is dominated by the area fraction and the survival rate is dominated by the failure strain. In the following sections, a more detailed analysis on how these two variables affect this phenomenon and further influence the failure of the composite will be presented.

3.2 Simulation Results

With area fraction (AF) from 0% to 60% and the failure strain of first network (EF) from 0.2% to 150%, 21 simulation cases were executed. Here AF and EF reflect the strength and stretchability of the first network in respect to the serpentine network. The loading curves from these simulations are grouped and presented with a focus on the failure strain and the fracture work of the composite to reflect both the individual and combined influences of AF and EF.

3.2.1 Different failure strain with fixed area fraction

Before looking at the combined effects of AF and EF, the individual influence of EF with a fixed AF is first evaluated. As shown in Fig. 3.2, the average reaction force is obviously increased with the increase of EF as a result of the significant increase in the

bottom forces and the minor increase in the peak forces. With such increases, the difference of the peak and bottom forces is reduced, which generates a more stable plateau during the damage propagation in first network. A noteworthy fact is that when EF increases from 0.2% to 50%, both the peak and bottom forces are drastically increased, which is not seen from the increase 50% to 100% and 100% to 150%.

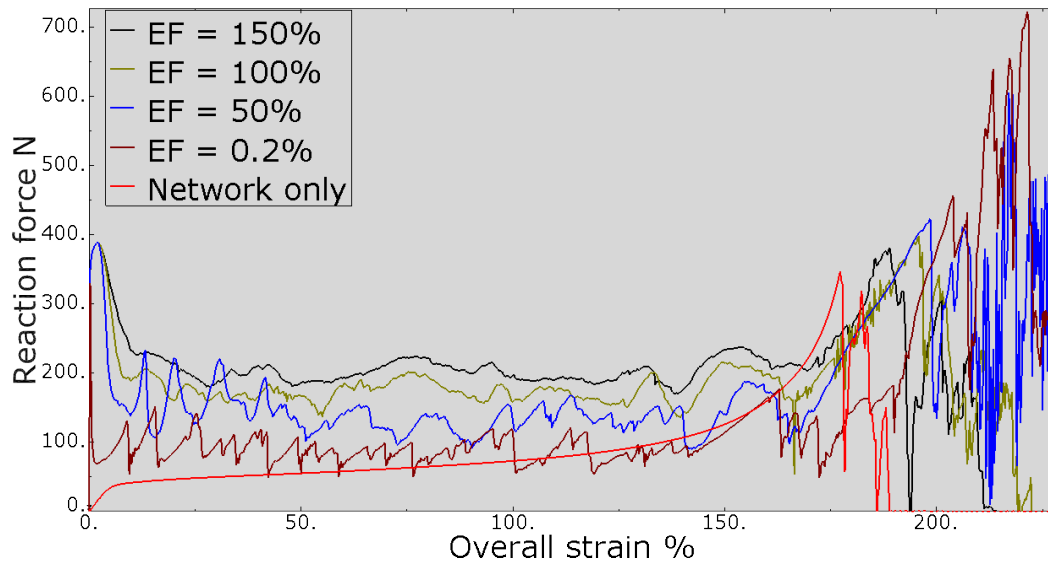


Fig 3.2 Loading curves with different failure strain of first network. Here the area fraction between the two components is fixed to be 23% and only the failure strain of first network (EF) is varied. A curve for serpentine network only is presented as a reference.

3.2.2 Different area fraction with fixed failure strain

Following the evaluation of EF influences, the analysis on the effects of different AFs when the same EF is executed. From the loading curve in Fig. 3.3, it can be observed that with an increased AF, the average reaction force also increases. However, different from the increased EF cases, the increase in reaction force is mainly induced by the prominent increase in peak forces. Besides, the bottom force is also slightly increased as a result of the

increase in AF. Another interesting fact to be mentioned is that although increasing the average force, the increased AF can cause the serpentine network fail to relocate the damage and result in a much reduced stretchability of the composite as shown by the AF = 47.3% curve in Fig. 3.3.

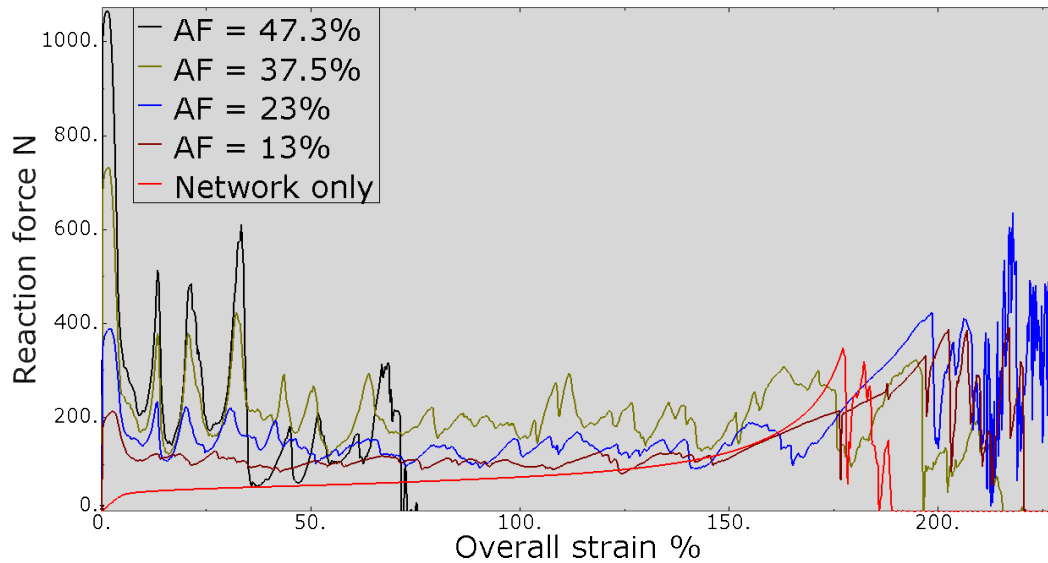


Fig. 3.3 Loading curves with different area fractions (AF). Here the failure strain of the second network is taken to be constant at 50% and AF is varied from 0% to 47.3%. To be noticed is that AF = 0% implies the serpentine network only case.

3.2.3 Combined area fraction and failure strain

To further evaluate the interaction of AF and EF and how they influence the composite together, two additional diagrams are established from the existing simulation results. The diagram one as shown in Fig. 3.4 (a), is the composite stretchability - EF diagram. Each curve in this diagram is drawn from a set of simulation results with a same AF. As shown in this diagram, most cases have a slightly better stretchability compared to the serpentine-only scenario. Meanwhile, as already suggested in Fig. 3.3, an overly high AF

causes a significant decrease in the failure strain of composite. However, a noteworthy phenomenon is that, the EF increase, although generally plays a small contribution to the stretchability decrease, actually brings the composite failure strain from below 100% back to over 200% in the AF = 47.3% set of simulation, which implies the increase of AF does change the effect of the increase of EF.

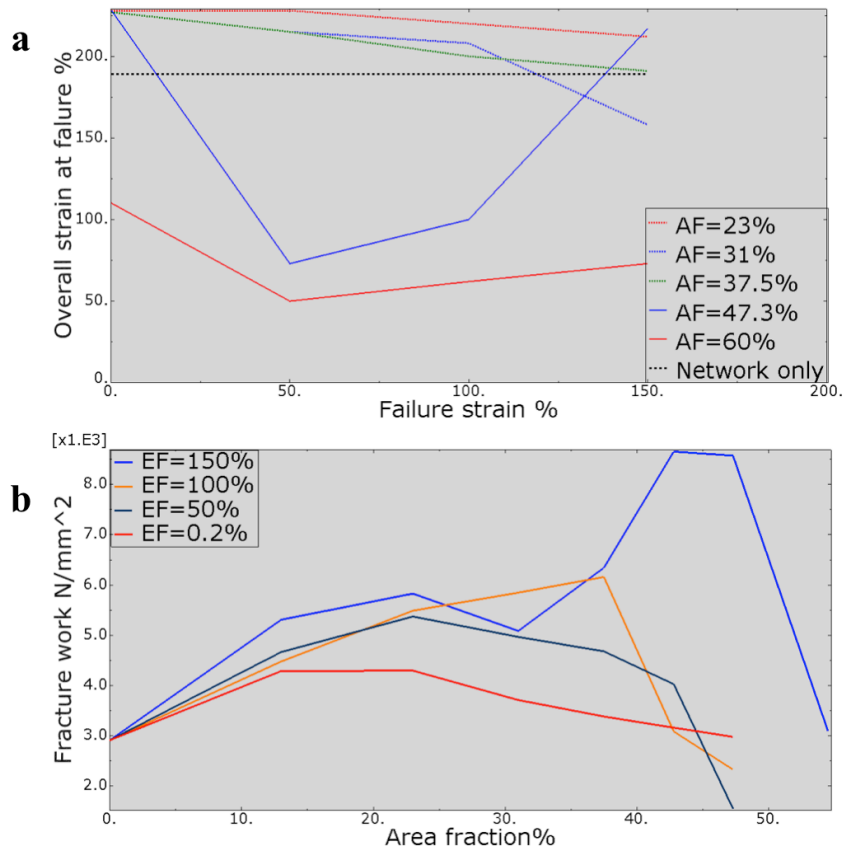


Fig. 3.4 (a) Composite failure strain - EF curves for different AF. Going from over 200 % to below 100% then back to over 200% as EF increases, the AF = 47.3% curve proves many things. (b) Fracture work per unit length - AF curves for different EF. The peak moves rightward with the increase of EF which denotes the EF and AF relationship.

Besides the composite failure strain - EF diagram, a fracture work per unit length - AF diagram is provided in Fig. 3.4(b). In this diagram, the fracture work is calculated as the

total work required to cause the failure of the structure divided by the total cross-sectional area of the composite and then further unified against the length of the composite. As reflected in the diagram, with a constant EF, the fracture work does not increase monotonically with AF and a peak fracture work appears in every curve. In addition, the AF generates the peak fracture work increases as the EF increases, which further confirms the fact that the effects of AF and EF would influence each other.

3.3 Concluding Results and Discussion

With the analysis of the damage process and the facts reflected in previous diagrams, a qualitative explanation towards the influences of EF and AF are proposed with the results concluded into three failure types. When focus on the benefit of high EF, because of the inhomogeneous deformation distribution in this structure, a fraction of the first network is not damaged when the serpentine network ligaments in the damage zone is straightened and this fraction increases with a higher EF. Since the reaction force of the structure is the sum of the reaction forces in both first and second network, the increase in undamaged first network increases the total reaction force of the bottom part, which appears when the serpentine ligaments are straightened and directly loaded. Conversely, with a very limited EF 0.2%, the first network is only partially loaded when a crack is initiated, therefore the peak force decreases obviously as a result of the decrease in first network reaction force during damage initiation. On the other hand, it is obvious that the increase in AF means a stronger first network, and therefore the reaction force required to relocate the damage to undamaged area is increased. As a result of this increase, the serpentine ligaments linking first network islands

are further straightened and heavier loaded, which causes every strip of the serpentine network is fully straightened and therefore the overall failure strain of the composite is even higher than that of the serpentine network only.

While in the previous discussion the benefits of increasing AF and EF are well stated, it is also important to understand the negative impact of the increases. As mentioned in previous section, when AF is too high, the first network is exceedingly strong causing the serpentine ligaments can not generate enough reaction force to relocate the damage. Therefore the failure type for such kind of bad design is named as the damage localization type of failure. During the fracture process of this failure type, after a damage initiation, the serpentine ligaments in the damage zone would be straightened and break as shown in Fig. 3.5.

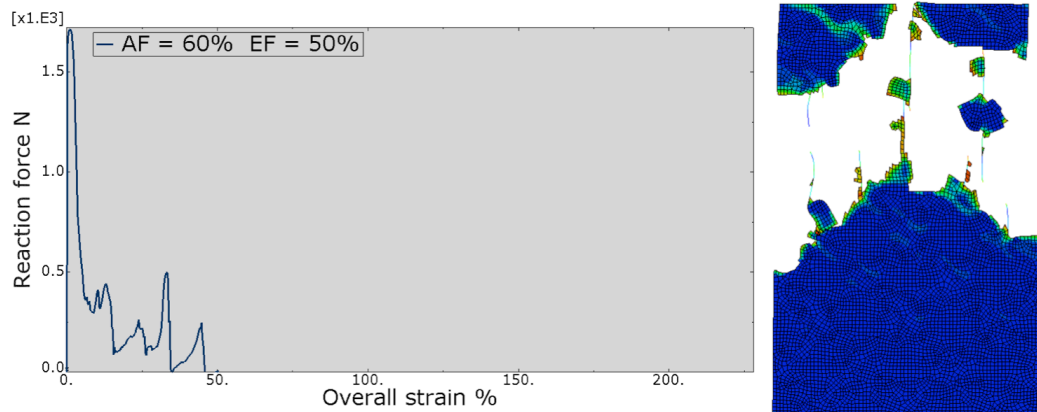


Fig. 3.5 The loading curve and failed result for damage localization type of failure. As can be observed from the result on the right, the serpentine ligaments in the damage zone is fully straightened but fail to initiate another crack.

Meanwhile, with a high EF, much of the first network would not be damaged at the end of local damage initiation, and these survived first network will strengthen the serpentine

network. As a result of the strengthening, the serpentine network may not need to be fully straightened to initiate another crack, therefore when the structure fails, the situation is as presented in Fig. 3.6, where only a minor portion of the serpentine ligaments are straightened and the stretchability of the composite is not as high. Accordingly, the results from similar are concluded as the pre-mature type of failure.

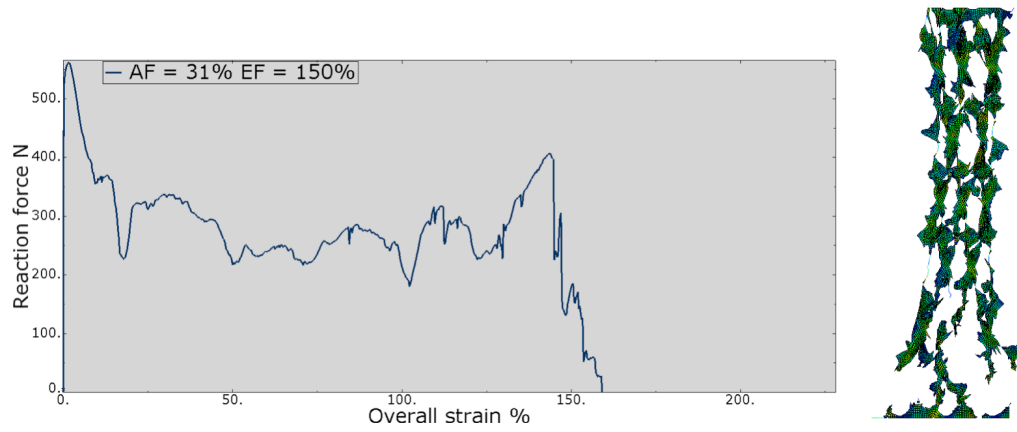


Fig. 3.6 The force-strain curve and the snapshot at the failure point for the composite with a pre-mature type of failure. As can be observed from the snapshot, many first network fragments are still remained on the serpentine network and the ligaments covered by these fragments are not straightened.

However, as can be concluded from statements above, the benefit of high AF would actually cancel the disadvantage from high EF and vice versa. More specifically, although a high EF would cause the remaining first and second network from damage zone induce the crack in undamaged area before the serpentine network is straightened, a stronger first network with the same EF would require the serpentine ligaments to be further straightened. Similarly, despite the fact that serpentine network may not be strong enough to relocate the

damage in first network, a higher EF would allow more first network to survive the local damage and compensate the required force.

To further support this statement, three simulation cases are selected: the AF = 47.3% EF = 50% case belongs to the damage localization type of failure and the AF = 31% EF = 150% belongs to the pre-mature type of failure and the case with AF = 47.3% EF = 150%. From Fig. 3.6, it is obvious that although AF = 47.3% and EF = 150% both induces undesired type of failure when the other parameter is not high enough, these two parameter actually balances each other and the corresponding case generates a high and stable plateau reaction force while maintaining a good stretchability.

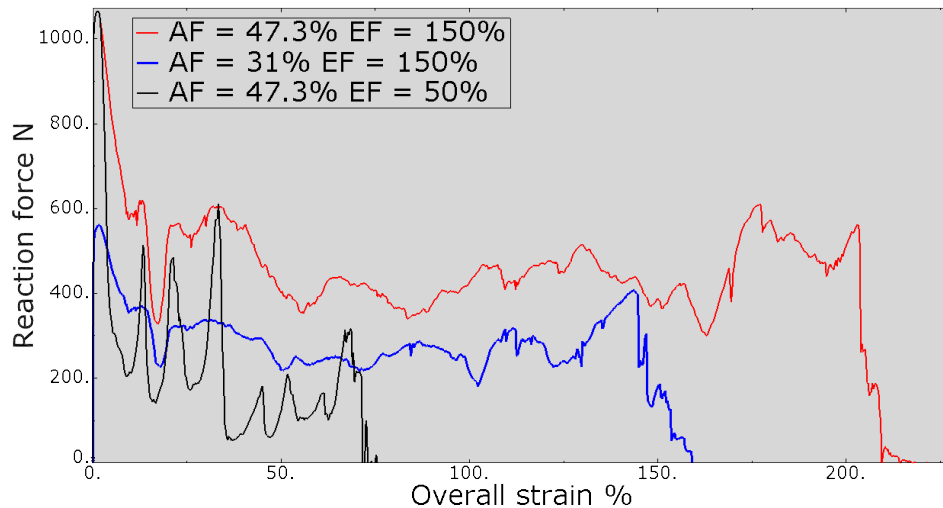


Fig. 3.7 Loading curve of three different of type of failure. The two curve at the bottom are both undesired result.

At this moment, it can be confirmed that the EF and AF would balance the negative impact of the other one and an optimized design requires balanced EF and AF to fully utilize the corresponding advantages. In such a design, the damage is well distributed in the first

network, and the serpentine network is fully straightened during the process of damage propagation so that the required fracture work is also much increased, which agrees with result in Fig. 3.4(b). Therefore the failure type for these cases are called the damage distribution type of failure and it is the desired failure type.

CHAPTER 4. CONCLUSION AND FUTURE WORK

4.1 Conclusion

At this point it can be concluded that, by introducing a serpentine network structure, the toughening mechanism of double-network hydrogel can also be applied to non-polymeric composites. With an optimized composition, the composite possess the high stretchability provided by the serpentine structure while still maintain a reasonable mechanical strength. During the fracture process, the damage in first network is continuously relocated to undamaged area by the second network until the first network is fully broken and a relatively stable plateau appears in the loading curve accordingly, which shows a high similarity to the fracture process of the hydrogels. The different composite compositions are well described by two dimensionless variables, the failure strain EF and area fraction AF , to cover possible stretchability and strength relationships. Through influencing the inhomogeneous deformation in first network, a higher EF stabilizes the plateau stress and postpones the damage localization in first network but may lead to pre-mature type of failure when too high. On the other hand, a higher AF increases the plateau stress and contribute to the prevention of pre-mature failure of second network but a overly high AF would result in the damage localization in first network. Therefore an optimized design is achieved through balancing the failure strain and strength of the first network material when the second network is fixed.

4.2 Possible Future Work

The possible future works of this research can be separated into two aspects. The first aspect is that, as a numerical simulation major based on idealized model, this research may involve experimental component to further verify and support the result from simulations. The second aspect is although the model proposed in this research focuses on two important variables that can well describe the composite composition, it sacrifices part of its accuracy in skipping many other important factors which can also be concluded into two groups. For the first network, its material model is a much simplified perfect plastic model which fails to capture the plastic hardening of the metallic material and the plastic hardening is actually an important part of the metal material model, therefore in the possible future work, the plastic hardening should be involved for better accuracy. For the second network, more configurable material structure with high stretchability can be applied to the second network and the detailed tuning of the existing serpentine network structure should also be carried out. Besides the geometry, further tests on the influence of second network material model should be conducted to confirm the applicability of making it constant.

REFERENCES

- [1] Gong, J.P., Katsuyama, Y., Kurokawa, T. and Osada, Y., 2003. Double-network hydrogels with extremely high mechanical strength. *Advanced Materials*, 15(14), pp.1155- 1158.
- [2] Gong, J.P., 2010. Why are double-network hydrogels so tough? *Soft Matter*, 6(12), pp. 2583-2590.
- [3] A. Rakovsky, D. Marbach, N. Lotan and Y. Lanir, *J. Appl. Polym. Sci.*, 2009, 112, 390.
- [4] C. Azuma, K. Yasuda, Y. Tanabe, H. Taniguro, F. Kanaya, A. Nakayama, Y. M. Chen, J. P. Gong and Y. Osada, *J. Biomed. Mater. Res., Part A*, 2006, 81, 373..
- [5] B. J. DeKosky, N. H. Dormer, G. C. Ingalve, C. H. Roatch, J. Lomakin, M. S. Detamore and S. H. Gehrke, *Tissue Eng., Part C*, 2010, 16, 1533.
- [6] Na, Y. H., Tanaka, Y., Kawauchi, Y., Furukawa, H., Sumiyoshi, T., Gong, J. P., & Osada, Y. (2006). Necking phenomenon of double-network gels. *Macromolecules*, 39(14), 4641-4645.
- [7] Webber, R. E., Creton, C., Brown, H. R., & Gong, J. P. (2007). Large strain hysteresis and mullins effect of tough double-network hydrogels. *Macromolecules*, 40(8), 2919-2927.
- [8] Y. Tanaka, K. Fukao and Y. Miyamoto, *Eur. Phys. J. E*, 2000, 3, 395
- [9] Lake GJ and Thomas AG. *Proceedings of the Royal Society of London Series a-Mathematical and Physical Sciences* 1967;300(1460):108-119.
- [10] Y. Tanaka, *Europhys. Lett.*, 2007, 78, 56005.
- [11] Hugh R. Brown, A Model of the Fracture of Double-network Gels , *Macromolecules*, 2007, 40 (10), pp 3815–3818
- [12] Wang, X. and Hong, W., 2011. Pseudo-elasticity of a double-network gel. *Soft Matter*, 7(18), pp.8576-8581.
- [13] B. D. Viers, J. E. Mark, *J. Macromol. (2007) Sci. Part A Pure Appl. Chem.* 44, 131–138.
- [14] G. D. Genesky, C. Cohen, (2010) *Polymer (Guildf.)* 51, 4152–4159 .
- [15] G. D. Genesky, B. M. Aguilera-Mercado, D. M. Bhawe, F. A. Escobedo, C. Cohen,

(2008) *Macromolecules* 41, 8231–8241 .

[16] N. K. Singh, A. J. Lesser, (2011) *Macromolecules* 44, 1480–1490 .

[17] E. Duocrot, Y. Chen, M. Bulters, R. P. Sijbesma, C. Creton (2014) Toughening elastomers with sacrificial bonds and watching them break, *Science* vol.344, pp. 186 - 189

[18] X. Feng, Z. Ma, J. V. MacArthur, C. J. Giuffre, A. F. Bastawros, W. Hong, 2016, *Soft Matter*, 2016,12, pp. 8999-9006

[19] J.-H. Lee, J. P. Singer, E. L. Thomas, *Adv. Mater.* 2012, 24, 4782.

[20] Q. Zhao, L. Kang, B. Du, B. Li, J. Zhou, H. Tang, X. Liang, B. Zhang, *Appl. Phys. Lett.* 2007, 90, 011112.

[21] K. Bi, Y. Guo, X. Liu, Q. Zhao, J. Xiao, M. Lei, J. Zhou, *Sci. Rep.* 2014, 4, 4139.

[22] I. V. Shadrivov, P. V. Kapitanova, S. I. Maslovski, Y. S. Kivshar, *Phys. Rev. Lett.* 2012, 109, 083902.

[23] J. Y. Ou, E. Plum, L. Jiang, N. I. Zheludev, *Nano Lett.* 2011, 11, 2142.

[24] S. Babae, J. Shim, J. C. Weaver, E. R. Chen, N. Patel, K. Bertoldi, *Adv. Mater.* 2013, 25, 5044.

[25] A. C. Steven, S. David, *New J. Phys.* 2007, 9, 45.

[26] S. Zhang, L. Yin, N. Fang, *Phys. Rev. Lett.* 2009, 102, 194301.

[27] J. Mei, G. Ma, M. Yang, Z. Yang, W. Wen, P. Sheng, *Nat. Commun.* 2012, 3, 756.

[28] X. Zheng, H. Lee, T. H. Weisgraber, M. Shusteff, J. DeOtte, E. B. Duoss, J. D. Kuntz, M. M. Biener, Q. Ge, J. A. Jackson, S. O. Kucheyev, N. X. Fang, C. M. Spadaccini, *Science* 2014, 344, 1373.

[29] J. Paulose, B. G.-G. Chen, V. Vitelli, *Nat. Phys.* 2015, 11, 153.

[30] M. Schenk, S. D. Guest, *Proc. Natl. Acad. Sci. USA* 2013, 110, 3276.

[31] J. L. Silverberg, A. A. Evans, L. McLeod, R. C. Hayward, T. Hull, C. D. Santangelo, I. Cohen, *Science* 2014, 345, 647.

- [32] T. Castle, Y. Cho, X. Gong, E. Jung, D. M. Sussman, S. Yang, R. D. Kamien, *Phys. Rev. Lett.* 2014, 113, 245502.
- [33] M. K. Bles, A. W. Barnard, P. A. Rose, S. P. Roberts, K. L. McGill, P. Y. Huang, A. R. Ruyack, J. W. Kevek, B. Kobrin, D. A. Muller, P. L. McEuen, *Nature* 2015, 524, 204.
- [34] T. C. Shyu, P. F. Damasceno, P. M. Dodd, A. Lamoureux, L. Xu, M. Shlian, M. Shtein, S. C. Glotzer, N. A. Kotov, *Nat. Mater.* 2015, 14, 785.
- [35] Z. Ma, X. Feng, W. Hong, Fracture of soft elastic foam *J. Appl. Mech* 83(3), 031007 (Dec 10, 2015)
- [36] Y. Cho, J.-H. Shin, A. Costa, T. A. Kim, V. Kunin, J. Li, S. Y. Lee, S. Yang, H. N. Han, I.-S. Choi, D. J. Srolovitz, *Proc. Natl. Acad. Sci. USA* 2014, 111, 17390.